HHS Public Access

Author manuscript

J Neuroimmunol. Author manuscript; available in PMC 2016 September 15.

Published in final edited form as:

J Neuroimmunol. 2015 September 15; 286: 16–24. doi:10.1016/j.jneuroim.2015.07.001.

The Intracerebroventricular injection of rimonabant inhibits systemic lipopolysaccharide-induced lung inflammation

Arnold Johnson, **Paul H. Neumann**, **Jianya Peng**, **Janey James**, **Vincenzo Russo**, **Hunter MacDonald**, **Nancy Gertzberg**, and **Carlos Feleder**

Department of Pharmaceutical Sciences, Albany College of Pharmacy and Health Sciences

Abstract

We investigated the role of intracerebroventricular (ICV) injection of rimonabant (500 ng), a CB_1 antagonist, on lipopolysaccharide ((LPS) 5mg/kg)-induced pulmonary inflammation in rats in an isolated perfused lung model. There were decreases in pulmonary capillary pressure (Ppc) and increases in the ((Wet-Dry)/Dry lung weight)/(Ppc) ratio in the ICV-vehicle/LPS group at 4 hours. There were decreases in TLR4 pathway markers, such as interleukin receptor-associated kinase-1, IκBα, Raf1 and phospho-SFK(Tyr416) at 30min and at 4hr increases in IL-6, vascular cell adhesion molecule-1 and myeloperoxidase in lung homogenate. Intracerebroventricular rimonabant attenuated these LPS-induced responses, indicating that ICV rimonabant modulates LPS-initiated pulmonary inflammation.

Graphical abstract

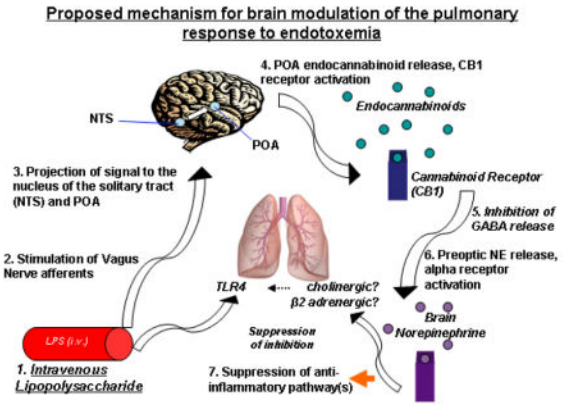

Corresponding Author: Carlos Feleder, MD, PhD, Associate Professor of Pharmaceutical Sciences, Department of Pharmaceutical Sciences, Albany College of Pharmacy and Health Sciences, 9 Samaritan Dr., BRB 104D, Albany, NY 12208, Tele: 518-694-7230, Fax: 518-694-7499, carlos.feleder@acphs.edu.

Conflicts of Interest

There is no conflict of interest.

Keywords

CB_1 receptor; rimonabant; pulmonary edema; lipopolysaccharide; TLR4; inflammation

1. Introduction

Sepsis has been generally understood as a complex intense systemic inflammatory response due to an infection (Angus et al., 2001, Dellinger et al., 2013, Hotchkiss and Karl, 2003, Van Amersfoort et al., 2003). The body's acute response to microbial components results in a widespread activation of cells. This causes a plethora of inflammatory mediators such as cytokines (e.g., cytokine storm), chemokines, prostaglandins, lipid mediators and reactive oxygen/nitrogen species to be released (Angus et al., 2001, Dellinger et al., 2013, Hotchkiss and Karl, 2003, Van Amersfoort et al., 2003). The aforementioned mediators induce systemic vasodilatation and upregulation of adhesion molecules in endothelium associated with the release, activation and organ sequestration of neutrophils and monocytes (Angus et al., 2001, Dellinger et al., 2013, Hotchkiss and Karl, 2003, Van Amersfoort et al., 2003). These changes in homeostasis subsequently lead to multiple organ failure such as acute lung injury, myocardial suppression and irreversible hypotension (Angus et al., 2001, Van Amersfoort et al., 2003).

Lipopolysaccaride (LPS) is used to model the effects of gram negative sepsis (Villanueva et al., 2009, Yilmaz et al., 2008a, Yilmaz et al., 2008b). Although the initiation and progression of LPS hypotension has been explained exclusively as a peripheral event, recent data from our laboratory showed that this effect of LPS can be prevented by (i) inhibiting the vagus nerve, (ii) by blocking neuronal activity in the nucleus of the solitary tract (NTS), (iii) by blocking α-adrenergic receptors in the preoptic area/anterior hypothalamic area (POA) and (iv) by blocking brain cannabinoid 1 receptors (CB_1) (Villanueva et al., 2009, Yilmaz et al., 2008a, Yilmaz et al., 2008b). These findings suggest that an inflammatory signal is conveyed from the periphery to the brain and the response to endotoxic shock is mediated through a central mechanism (Villanueva et al., 2009, Yilmaz et al., 2008a, Yilmaz et al., 2008b). Importantly, recent studies show that treatment in the brain with the CB_1 receptor inverse agonist/antagonist, rimonabant, prior to endotoxemia, decreases systemic tumor necrosis factor α (TNF-α) levels, central norepinephrine concentrations within the POA, and prevents endotoxic hypotension (Villanueva et al., 2009).

Lung inflammation with the resultant acute respiratory distress syndrome (ARDS) is an additional characteristic outcome of severe endotoxemia (Van Amersfoort et al., 2003, Gando et al., 2004). However, the role of the CB_1 receptors in the brain in the modulation of lung inflammation during endotoxemia has not been studied. Many brain areas, including the hypothalamus, contain CB_1 receptors (Matsuda et al., 1993, Hirasawa et al., 2004, Herkenham et al., 1991). Furthermore, CB_1 receptors can modulate the autonomic nervous system, and therefore, bidirectional circuits between the periphery and the brain (Schulte et al., 2012). Particularly, neurons which are involved in the response to endotoxin (Ibrahim and Abdel-Rahman, 2011, Lee et al., 2010).

Toll-like receptor 4 (TLR4) is a critical receptor for recognition of LPS in many cell types, including endothelial cells (Faure et al., 2000) and is unique among toll-like receptors in having both myeloid differentiation primary response 88 (MyD88) -dependent and MyD88-independent signaling pathways (Vogel et al., 2003). The MyD88-dependent signaling pathway is initiated first upon TLR4 activation followed by later MyD88-independent signaling, after TLR4/LPS/CD14 endosomal internalization (Kagan et al., 2008). Interleukin receptor-associated kinase-1 (IRAK1) is an essential upstream effector of TLR4 signaling in the MyD88-dependent pathway and required for MyD88-dependent NFκB pathway activation. Upon activation, IRAK1 is hyperphosphorylated and then undergoes proteasomal degradation (Kawagoe et al., 2008). Inactive NFκB resides in quiescent cells associated with its inhibitor of κB (IκBα). Upon activation, IκBα is phosphorylated, releasing NFκB for phosphorylation, nuclear translocation and gene regulatory effects while the phospho-IκBα undergoes proteasomal degradation (Faure et al., 2000).

Early signaling events of TLR4 also include Src family kinase (SFK: src, lyn, fyn, and yes) activation and a Raf1/MAPK pathway activation. The LPS-induced TLR4 activation of SFKs is MyD88-dependent, involving TNFα receptor-associated factor 6 (TRAF6) interaction with IRAK, ultimately leading to increased endothelial permeability through SFK phosphorylation of adherens junction proteins (Gong et al., 2008, Liu et al., 2012). Raf1, which contains a SFK activation site (Fabian et al., 1993), has been shown, through the Ras/Raf1/MEK/ERK pathway to be involved with phosphatidyl-inositol-3-kinase (PI3-K) phosphorylation, regulation of NFκB activation, and upregulation and expression of tissue factor (TF) and TNFα (Nakayama et al., 2003, Guha et al., 2001).

Later effects of TLR4 signaling include the upregulation of cytokines, chemokines, intercellular adhesion molecules, inducible nitric oxide synthase (iNOS), and other mediators of inflammation (Arroyo-Espliguero et al., 2004). The vascular cell adhesion molecule, (VCAM-1) (Sawa et al., 2008), myeloperoxidase (MPO) (Su et al., 2010), and IL-6 (Birukova et al., 2012, Simons et al., 1996), are markers of inflammation and participate in lung injury.

The aim of this study is to determine if ICV rimonabant modulates the lung's hemodynamic and inflammatory response to LPS via modulation of TLR4 signaling.

2. Materials and Methods

2.1 Reagents

All reagents are obtained from Sigma Chemical Company (St. Louis, MO) unless otherwise noted.

2.2 Brain injection and treatments

These animal studies were approved by the Institutional Animal Care and Use Committee and the care and handling of the animals were in accord with National Institutes of Health guidelines.

Male Sprague-Dawley rats (200 – 220 g; Charles River Laboratories, Wilmington, Mass) were anesthetized with a cocktail consisting of Ketamine HCL (80 mg/kg), Xylazine (5.0 mg/kg), and Acepromazine (1.0 mg/kg) administered intraperitoneally (IP) at 2.0 ml/kg. The anesthetic was administered as needed to maintain the appropriate level of anesthesia throughout the procedure. Body temperature was kept constant with a heating pad (Adroit, Braintree Scientific, Braintree, MA). Animals were monitored throughout all procedures for respiration and level of anesthesia. For intracerebroventricular (ICV) injections, the needle of a 10 µl Hamilton syringe was lowered through a burr hole drilled through the skull with its tip 4.0 mm below the surface of the skull, 1.5 mm lateral and 0.5 mm posterior to the bregma. The endocannabinoid receptor inverse agonist/antagonist rimonabant (Villanueva et al., 2009) (500 ng in 0.5 µl saline + 2.5% DSMO) or saline/DMSO alone was injected ICV 5 minutes prior to IV injection of LPS or saline (30 minute and 4 hour studies) with additional ICV injections 1.5 and 3 hours post-IV injection in 4 hour studies. The rats were given a tail vein injection of either LPS (5 mg/kg) or 0.9% saline (1ml/kg) 5 minutes after the baseline ICV injection of rimonabant. At the end of the study each rat was sacrificed, the brain removed, frozen on dry ice, and sections of 50µM were cut with a microtome cryostat (Microcom Model HM505E, Waldorf, Germany). Sections were mounted on slides, stained with eosin, air dried and coverslipped, and the location of the needle tip was confirmed (Feleder et al., 2007). Only the data from confirmed placement was considered.

2.3 Study groups

Treatment		
	30 minutes	**N**
Control	(vehicle ICV / vehicle IV)	8
LPS	(vehicle ICV / LPS IV)	9
Rimonabant	(rimonabant ICV / vehicle IV)	8
Rimonabant + LPS	(rimonabant ICV / LPS IV)	5
IV Rimonabant + LPS	(rimonabant IV / LPS IV)	3
	4 hours	
Control	(vehicle ICV / vehicle IV)	5
LPS	(vehicle ICV / LPS IV)	10
Rimonabant	(rimonabant ICV / vehicle IV)	6
Rimonabant + LPS	(rimonabant ICV / LPS IV)	5

2.4 Lung isolation

The trachea was cannulated (2.42mm diameter polyethylene tubing) and the chest was opened by median sternotomy 30 minutes or 4 hours after the LPS injection. Heparin (7 U/10 g body weight, Abraxis Pharmaceutical, Schaumberg, IL) was administered by intracardiac puncture injection. The lungs and heart were excised and the pulmonary artery and left atrium were cannulated. The lungs and heart were then suspended from a force displacement transducer (model TSD105A, Harvard Apparatus, Holliston, MA) and perfusion was begun within 5 min of excision.

The lungs were ventilated with room air using a small animal ventilator (CWE, Ardmore, PA) set at 60 bpm and 2 ml tidal volume. Lung perfusion (0.04 ml/min/g body weight) was maintained by a peristaltic roller perfusion pump (model 7523–60, Cole-Palmer, Vernon Hills, IL). The circulation of perfusate (150 ml of phosphate buffered Ringer's solution with 5.55 mM dextrose and 3.0 g/100 ml bovine serum albumin (fraction V)) (Ringer's/BSA) was used to clear intravascular cellular elements. The system was maintained at a constant temperature of 37 °C, and pH 7.4. The pulmonary artery pressure (Ppa) and the pulmonary venous pressure (Ppv) were monitored using catheters (PE-50) inserted into the pulmonary artery and left atrial appendage, respectively, and connected to a pressure transducer (model TSD104A, Harvard Apparatus). Pressures were recorded continuously (model MP100 w/ Acknowledge Software, BioPac Systems, Inc., Goleta, CA). The Ppv was maintained at 2.9 mmHg throughout the experiment. Pulmonary capillary pressure (Ppc) was estimated using the double occlusion method as previously described (Johnson and Ferro, 1996), measured in triplicate during the perfusion period of 25–45 min.

Left lungs were weighed in their wet state after perfusion and subsequently oven dried for three days. The left lung wet to dry ratio was calculated by [(wet weight – dry weight)/dry weight] ((W-D)/D) to remove the tissue weight from the calculation and measure only fluid weight (Barton-Pai et al., 2011). The right lung was immediately diced into ~3 mm pieces, frozen in liquid nitrogen, and stored at −80 °C for later homogenization for western blot analysis.

2.5 Lung homogenization

Frozen lung tissue was homogenized on ice with a Bio homogenizer M 33/1281–0 (Biospec Products, Inc., Bartlesville, OK) in 16 ml polycarbonate centrifuge tubes (Sorvall No. 03243, DuPont, Wilmington, DE). Between 150 to 200 mg tissue was homogenized at high speed for 45 s in homogenization buffer (Tris HCl: 10 mM-pH 7.5; SDS: 0.1%; Triton X-100: 0.5%; Sodium Deoxycholate: 0.5%; DTT: 0.5 mM) supplemented with 2x mammalian protease inhibitor and phosphatase inhibitor 2 and 3 cocktails *(#P8340, #P5726, #P0044, Sigma)* at 1 ml/100 mg tissue. Aliquots of homogenate were centrifuged at 36,000×g, 4 °C for 60 min and supernatants were normalized to 2.5 μg/ml following protein determination with the BCA assay (Thermo Scientific, Rockford, Il). Aliquots of normalized supernatant were prepared for SDS-PAGE by addition of 5x Laemmli buffer and incubation at 95 °C for 10 min.

2.6 Immunoblots

Protein identification using PAGE-Western Blot was done with adaptations of previously described techniques from this laboratory (Barton-Pai et al., 2011, Pai et al., 2012). Lung homogenates, 20 μg/lane, were separated on 9–18% gradient and 8.75% polyacrylamide minigels, transferred to PVDF membranes, blocked, and probed overnight at 4°C. The primary antibodies used were anti-IRAK1, anti-IL-6, anti-VCAM (sc-7883, sc-1265-R, sc-1504, Santa Cruz Biotechnology, Santa Cruz, CA), anti-IκBα, anti-phospho-IκBα(Ser32/36), anti-myeloperoxidase, anti-phospho-Src Family kinase(Tyr416), anti-Src, and anti-Raf1 (#4814, #9246, #4162, #6943, #2123, #9422, Cell Signaling Technology, Danvers, MA), followed by secondary incubation with bovine anti-rabbit-HRP, bovine anti-

goat-HRP (sc-2374, sc-2352, Santa Cruz), or goat anti-mouse-HRP (#A8924, Sigma) as appropriate. Blots were stripped with Restore PLUS Western Blot Stripping Buffer (Thermo Scientific), and the imaging substrates used were Supersignal West Pico or West Dura Extended Duration Substrate (Thermo Scientific) or a combination of the two. Images were acquired on a Chemidoc XRS (Bio-Rad, Hercules, CA) and net band intensity units were measured with Image Lab image analysis software (Bio-Rad).

2.7 Statistics

A one way analysis of variance (ANOVA) was used to compare values among the treatments. If significance among treatments was noted, a post-hoc multiple comparison test was done with a Bonferoni test to determine significant differences among the groups. A Student T-Test was performed when appropriate. Each lung represents a single experiment. All data are reported as mean ± S.E.M. Significance was at $P<0.05$.

3. Results

3.1 Pulmonary hemodynamics and edema

The effect on pulmonary capillary pressure after a 30 minute or 4 hour exposure to systemic LPS in the presence or absence of ICV rimonabant treatment is shown in Figure 1A. There was a significant decline in Ppc at 4 hours post-LPS, which did not occur with prior ICV injection followed by two subsequent post-LPS ICV injections of 500 ng rimonabant. Preliminary studies using a single dose of 250 or 500 ng of rimonabant ICV showed no protective effect 4 hours post-LPS (data not shown), possibly as a result of its relatively short half-life. The ICV injection of rimonabant alone had no effect. The dose of rimonabant selected is extremely low and insufficient to affect LPS induced lung inflammation when injected systemically (Villanueva et al., 2009, Kadoi and Goto, 2006, Varga et al., 1998). The dose used here is also appropriate for blocking behavioral effects centrally (Laviolette and Grace, 2006).

These data indicate that endocannabinoid receptor blockade prevents the pulmonary hemodynamic effects of systemic LPS. Figure 1B shows the effect of a 30 minute or 4 hour exposure to systemic LPS on lung (W-D)/D weight ratio in the presence or absence of ICV rimonabant treatment. There was a trend toward increased lung (W-D)/D ratio in the LPS treated animals at 30 minutes that became significant after 4 hours, which was prevented in rats treated with rimonabant. To account for the differential capillary pressure effect of LPS, the lung (W-D)/D ratio was normalized to Ppc (Figure 1C). Again, there was a slight increase in the ((W-D)/D) / Ppc ratio of the LPS treated animals at 30 minutes and a large increase after 4 hours, neither of which occurred in the rats treated with rimonabant. These data indicate that endocannabinoid receptor blockade prevents pulmonary fluid accumulation following systemic LPS injection.

3.2 TLR4 signaling

Western blots were generated from the supernatants of lung homogenates from animals exposed for 30 minutes to a systemic LPS dose with or without ICV rimonabant pretreatment. Representative blots of IRAK1 (upper band), phospho-IκBα$^{Ser32/36}$ (middle

band), and IκBα (lower band) are shown in Figure 2A. The relative band density units (RDU) for IRAK1 generated from all such blots are shown in Figure 2B. LPS caused a significant decrease in IRAK1, indicating TLR4-induced IRAK1 activation and degradation, which was prevented in rats pretreated with ICV rimonabant. The IRAK1 antibody used here detects only the inactive non-hyperphosphorylated protein. The data of Figure 2B suggests ICV rimonabant pretreatment may initiate inhibition of the MyD88-dependent pathway and/or a significant drop in proteasomal degradation along with dephosphorylation of activated IRAK1. The RDU for phospho-IκBα$^{Ser32/36}$ generated from all such blots are shown in Figure 2C. LPS caused a significant increase in pIκBα$^{Ser32/36}$, indicating TLR4/NFκB pathway activation, which was not prevented in rats pretreated with ICV rimonabant. The RDU for total IκBα generated from the blots are shown in Figure 2D. LPS caused a significant decrease in IκBα indicating degradation of phospho-IκBα. However, this decrease in IκBα was entirely eliminated in the LPS group pretreated ICV with rimonabant. The IκBα antibody used here binds the protein independent of its phosphorylation state. Given the equal phosphorylation levels of IκBα shown in Figure 2C following IV LPS, despite rimonabant pre-treatment, the data of Figure 2D indicates a significant drop in proteasomal degradation of pIκBα$^{Ser32/36}$ in the ICV rimonabant pre-treated group.

Representative Western blots of phospho-SFK^{Tyr416} (top band), total Src (second band), total Raf1 (third band), and total β-actin (lower band) are shown in Figure 3A. The RDU for phospho-SFK^{Tyr416} generated from all such blots are shown in Figure 3B. LPS induced a significant decrease in the constitutive level of phospho-SFK^{Tyr416}, indicating a reduction in activation, which was prevented by ICV pre-treatment with rimonabant. The RDU for Raf1 generated from the blots are shown in Figure 3C. LPS caused a significant decrease in the constitutive level of Raf1, which was prevented in the LPS group pretreated ICV with rimonabant. The data of Figure 3C indicates a significant drop in proteasomal degradation of RAF1 in the ICV rimonabant pre-treated group. The blots of total Src and β-actin indicate equal gel protein loading. The data in Figures 2 and 3 indicate that endocannabinoid receptor blockade with rimonabant alters the LPS-induced changes in mediators proximal to TLR4 signaling, further supporting the hypothesis that central CB_1 receptor activity modulates TLR4 signaling in the lung.

3.2 Intravenous Rimonabant

Systemic IV, as opposed to ICV, pretreatment with rimonabant (5 minutes, 500 ng/0.5μl) did not affect the LPS-induced changes described above in TLR4 signaling (Figure 4). Western blots were generated from the supernatants of lung homogenates from animals exposed for 30 minutes to a systemic LPS dose with or without ICV or IV rimonabant pretreatment. Representative blots of IRAK1 (upper band), total IκBα (middle band), and β-actin (lower band) as well as the quantified band densities for IRAK1 and IκBα are shown in Figure 4A. LPS caused a significant decrease in both IRAK1 and IκBα which was not prevented by IV rimonabant. Representative blots of phospho-SFK^{Tyr416} (upper band), total Src (middle band), β-actin (lower band) and the band densities for phospho-SFK^{Tyr416} are shown in Figure 4B. LPS caused a significant decrease in phospho-SFK^{Tyr416} which was not prevented by IV rimonabant. Figure 4C shows blots of total RAF1 (upper band), β-actin

(lower band), and the band densities for RAF1. Intravenous administration of rimonabant did not prevent the LPS-induced decrease of total RAF1. The data in Figure 4 indicate that the modulating effect of rimonabant on the LPS-induced pulmonary response occurs solely through its action in the ICV and not the periphery.

3.4 Markers of pulmonary inflammation

Western blots were generated from the supernatants of lung homogenates from animals exposed for 4 hours to systemic LPS with or without ICV rimonabant pretreatment followed by additional ICV rimonabant treatments 1.5 and 3 hours post-LPS. Figure 4A shows representative Western blots of the IL-6, VCAM-1, and MPO in the 4 hour Control, Rimonabant, LPS, and LPS+Rimonabant treated groups. LPS induced a significant increase in the level of IL-6, which was prevented by ICV treatment with rimonabant, as shown in Figure 4B. Figure 4C shows a significant increase in VCAM-1 following LPS which was significantly reduced with rimonabant treatment. LPS induced a significant increase in the level of MPO, a marker of neutrophil sequestration, which was prevented by ICV treatment with rimonabant, as shown in Figure 4D. The data of Figure 4 supports the idea that LPS-induced lung inflammation is influenced by central antagonism of the CB_1 receptor.

4. Discussion

The present study shows that rimonabant, a CB_1 receptor antagonist, injected ICV inhibits lung inflammation induced by LPS. This effect is exerted by modifying TLR4 signaling cascade activation in the lung.

The mechanism for intra-cerebral protection of rimonabant binding on CB_1 receptors in the brain (Ando et al., 2012, Fride, 2002, Szabo and Schlicker, 2005) remains to be determined. We speculate that protection may be exerted by modulating a pathway that is centrally commanded by the brain through the autonomic nervous system, the sympathetic and/or the cholinergic systems (Rosas-Ballina and Tracey, 2009, Martelli et al., 2014b, Martelli et al., 2014a). Several areas of the brain including the hypothalamus express CB_1 receptors (Matsuda et al., 1993, Hirasawa et al., 2004, Herkenham et al., 1991) and project to a number of autonomic centers thus regulating sympathetic and vagal activity (Chiba and Murata, 1985, Saper et al., 1976, Lindberg et al., 2013, Cardinal et al., 2014, Nance and Sanders, 2007). β_2 adrenergic as well as $\alpha 7$ nicotinic acetylcholine receptors have shown to be involved in modulation of inflammation in the lung. Su et al., reported that both cholinergic $\alpha 7$ nicotinic acetylcholine receptors ($\alpha 7$nAChR) and β_2 adrenergic receptors modulate the lung response to LPS and E. coli (Su et al., 2010, Su et al., 2006), suggesting a crucial role for the autonomic system in this process. Therefore, this effect might be finally mediated by β_2 adrenergic receptors and/or cholinergic receptors that are located on immune, endothelial, epithelial, and vascular smooth muscle cells (Wang et al., 2001, Gu et al., 2013, Su et al., 2010, Su et al., 2006, Nance and Sanders, 2007, Bosmann et al., 2012) to modulate the TLR4 signaling pathway in the lung (Rosas-Ballina and Tracey, 2009, Su et al., 2010, Togbe et al., 2006). This hypothesis needs to be further explored.

The central nervous system may also modulate lung inflammation through the activation of the adrenal axis and release glucocorticoids that can inhibit the inflammatory response (Besedovsky et al., 1986)

This study shows for the first time that ICV rimonabant modulates the pulmonary hemodynamic and inflammatory response to IV LPS. Rimonabant is an inverse agonist/antagonist of brain endocannabinnoid CB_1 receptors, and has no effect on mu and delta opioid brain receptors (Kathmann et al., 2006). In the LPS group, there was a decrease in the Ppc which became significant at 4 hours. In that same group, there were increases in the (W-D)/D and ((W-D)/D)/Ppc lung weight ratios which indicate an increase in lung wet weight, independent of the Ppc. This increase in lung fluid despite the lower capillary pressure suggests an increase in pulmonary vascular permeability (Johnson and Ferro, 1996). Notably, the increase in the (W-D)/D and ((W-D)/D)/Ppc lung weight ratios did not occur in the ICV rimonabant treated groups.

The decrease in Ppc was previously observed in lungs from animals treated for 24 hours with TNFα intravenously (Barton-Pai et al., 2011). In the present study, the LPS-induced decrease in Ppc did not occur in the ICV rimonabant+IV LPS group. To examine the possibility of ICV rimonabant modulation of NO-induced dilation of lung post-capillary microvessels, levels of iNOS were measured, but were found to be identical in both IV LPS groups (Data not shown). This would suggest that the protective effect of rimonabant treatment is independent of iNOS levels and the mechanism for the unchanged Ppc remains to be determined.

In this study, ICV rimonabant pretreatment elicited a profound effect on two of the early signaling markers of canonical TLR4 activation: IRAK1 and IκBα. The activation of IRAK1 and phosphorylation of IκBα indicates LPS binding to the TLR4 receptor and activation of the downstream signaling response (Toubiana et al., 2010, Rosas-Ballina and Tracey, 2009, Togbe et al., 2006) which is associated with expression and/or release of inflammatory biomarkers such as VCAM and IL-6. The phosphorylation mediated activation of IRAK1 and IκBα results in their proteasomal degradation (Toubiana et al., 2010). Rimonabant pretreatment prevented the 30 minute LPS-induced decrease in IRAK1 and IκBα and yet had no apparent effect on the level of IκBα phosphorylation, however, phosphorylation of IkBa and activation of the NFkB pathway also occurs via the TLR4/MyD88 independent pathway. The prevention of degradation of IRAK1 could indicate a rimonabant induced inhibition of its upstream activators, MyD88/IRAK4, or an inhibition of its proteosomal degradation and a dephosphorylation to its inactive state. Indeed, both An et al. and Abu-Dayyeh et al. have reported inhibition of both kinase activity and degradation of IRAK1 following direct binding to it by the phosphatase SHP-1 (An et al., 2008, Abu-Dayyeh et al., 2008) and Dobierzewska et al. has reported dephosphorylation of IRAK1 by the phosphatase PP2A (Dobierzewska et al., 2011). The ICV rimonabant-induced prevention of IκBα degradation, despite its phosphorylation, more strongly suggests an inhibition of proteasomal degradation.

There was an increase in pulmonary VCAM, MPO and IL-6 at 4 hours post-LPS, suggesting sequestration, accumulation and extravasation of activated neutrophils and monocytes in the

lung. The sequestration can be caused by upregulation of neutrophil and monocyte adherence proteins in the lung such as VCAM (Lomakina and Waugh, 2009). Moreover, both neutrophils and monocytes express IL-6 which can explain the increase in lung IL-6 in the LPS group. Activated neutrophils and monocytes are associated with lung edema (Su et al., 2010) which is similar to the present result that LPS causes an increase in the (W-D)/D/Ppc ratio directly correlated with increased VCAM, MPO and IL-6. The increase in lung edema, MPO, IL-6 and VCAM was prevented in the ICV rimonabant treated animals. The inhibition of LPS-TLR4 signaling after rimonabant treatment could result in decreased NFkB dependent protein expression of phlogistic molecules such as IL-6 and VCAM, thus resulting in prevention of LPS-induced lung edema.

One caveat to these results is that these experiments were performed under ketamine and xylazine anesthesia, which may have influenced experimental outcomes. Ketamine has been described as an anti-inflammatory agent and xylazine suppresses sympathetic nerve activity (Busch et al., 2010, Madden et al., 2013). However, the present and previous studies performed in our lab and by others show an ample pulmonary inflammatory response to either LPS or TNFα despite using this anesthesia cocktail (Barton-Pai et al., 2011, Su et al., 2010, Su et al., 2006, Liaudet et al., 2002). This indicates that LPS can still induce inflammation and this response is not being prevented by the anesthesia cocktail. In addition, prior studies in which isoflurane anesthesia was utilized showed that rimonabant ICV inhibited LPS-induced hypotension. This result suggests the possibility of rimonabant interacting with the current ketamine and xylazine cocktail is unlikely (Villanueva et al., 2009).

5. Conclusion

In conclusion, the major original finding of the present study is that rimonabant acting in the brain inhibits LPS-induced lung inflammation, a foremost characteristic of endotoxemia. We also show that rimonabant modulates the lung TLR4 signaling cascade triggered by LPS.

These findings are potentially important for clinical investigators who seek new therapeutic strategies for preventing or treating endotoxic shock and related conditions. Indeed, the fact that blocking LPS-induced lung inflammation prevents the progression that often generates lung injury and death raises the possibility that endotoxic shock may be treated or prevented centrally with CB_1 receptor antagonists.

Acknowledgments

Source of Funding

Research Supported by NIH R15A1072744 to C. Feleder and NIH R01 HL059901 to A. Johnson.

Abbreviations used

ICV	intracerebroventricular
CB_1	cannabinoid receptor type 1

LPS	lipopolysaccharide
IV	intravenous
Ppc	pulmonary capillary pressure
TLR4	toll-like receptor 4
IRAK1	interleukin receptor-associated kinase-1
IκBα	inhibitor of nuclear factor of kappa light polypeptide gene enhancer in B-cells type alpha
NFκB	nuclear factor kappa-light-chain-enhancer of activated B cells
SFK	Src family kinase
IL-6	interleukin-6
VCAM-1	vascular cell adhesion molecule 1
MPO	myeloperoxidase

References

ABU-DAYYEH I, SHIO MT, SATO S, AKIRA S, COUSINEAU B, OLIVIER M. Leishmania-induced IRAK-1 inactivation is mediated by SHP-1 interacting with an evolutionarily conserved KTIM motif. PLoS Negl Trop Dis. 2008; 2:e305. [PubMed: 19104650]

AN H, HOU J, ZHOU J, ZHAO W, XU H, ZHENG Y, YU Y, LIU S, CAO X. Phosphatase SHP-1 promotes TLR- and RIG-I-activated production of type I interferon by inhibiting the kinase IRAK1. Nat Immunol. 2008; 9:542–50. [PubMed: 18391954]

ANDO RD, BIRO J, CSOLLE C, LEDENT C, SPERLAGH B. The inhibitory action of exo- and endocannabinoids on [(3)H]GABA release are mediated by both CB(1)and CB(2)receptors in the mouse hippocampus. Neurochem Int. 2012; 60:145–52. [PubMed: 22133429]

ANGUS DC, LINDE-ZWIRBLE WT, LIDICKER J, CLERMONT G, CARCILLO J, PINSKY MR. Epidemiology of severe sepsis in the United States: analysis of incidence, outcome, and associated costs of care. Crit Care Med. 2001; 29:1303–10. [PubMed: 11445675]

ARROYO-ESPLIGUERO R, AVANZAS P, JEFFERY S, KASKI JC. CD14 and toll-like receptor 4: a link between infection and acute coronary events? Heart. 2004; 90:983–8. [PubMed: 15310678]

BARTON-PAI A, FELEDER C, JOHNSON A. Tumor necrosis factor-alpha induces increased lung vascular permeability: a role for GSK3alpha/beta. Eur J Pharmacol. 2011; 657:159–66. [PubMed: 21316358]

BESEDOVSKY H, DEL REY A, SORKIN E, DINARELLO CA. Immunoregulatory feedback between interleukin-1 and glucocorticoid hormones. Science. 1986; 233:652–4. [PubMed: 3014662]

BIRUKOVA AA, TIAN Y, MELITON A, LEFF A, WU T, BIRUKOV KG. Stimulation of Rho signaling by pathologic mechanical stretch is a “second hit” to Rho-independent lung injury induced by IL-6. Am J Physiol Lung Cell Mol Physiol. 2012; 302:L965–75. [PubMed: 22345573]

BOSMANN M, GRAILER JJ, ZHU K, MATTHAY MA, SARMA JV, ZETOUNE FS, WARD PA. Anti-inflammatory effects of beta2 adrenergic receptor agonists in experimental acute lung injury. FASEB J. 2012; 26:2137–44. [PubMed: 22318967]

BUSCH CJ, SPOHR FA, MOTSCH J, GEBHARD MM, MARTIN EO, WEIMANN J. Effects of ketamine on hypoxic pulmonary vasoconstriction in the isolated perfused lungs of endotoxaemic mice. Eur J Anaesthesiol. 2010; 27:61–6. [PubMed: 19923994]

CARDINAL P, ANDRE C, QUARTA C, BELLOCCHIO L, CLARK S, ELIE M, LESTE-LASSERRE T, MAITRE M, GONZALES D, CANNICH A, PAGOTTO U, MARSICANO G, COTA D. CB1 cannabinoid receptor in SF1-expressing neurons of the ventromedial hypothalamus

determines metabolic responses to diet and leptin. Mol Metab. 2014; 3:705–16. [PubMed: 25352999]

CHIBA T, MURATA Y. Afferent and efferent connections of the medial preoptic area in the rat: a WGA-HRP study. Brain Res Bull. 1985; 14:261–72. [PubMed: 3995367]

DELLINGER RP, LEVY MM, RHODES A, ANNANE D, GERLACH H, OPAL SM, SEVRANSKY JE, SPRUNG CL, DOUGLAS IS, JAESCHKE R, OSBORN TM, NUNNALLY ME, TOWNSEND SR, REINHART K, KLEINPELL RM, ANGUS DC, DEUTSCHMAN CS, MACHADO FR, RUBENFELD GD, WEBB S, BEALE RJ, VINCENT JL, MORENO R. SURVIVING SEPSIS CAMPAIGN GUIDELINES COMMITTEE INCLUDING THE PEDIATRIC S. Surviving Sepsis Campaign: international guidelines for management of severe sepsis and septic shock, 2012. Intensive Care Med. 2013; 39:165–228. [PubMed: 23361625]

DOBIERZEWSKA A, GILTIAY NV, SABAPATHI S, KARAKASHIAN AA, NIKOLOVA-KARAKASHIAN MN. Protein phosphatase 2A and neutral sphingomyelinase 2 regulate IRAK-1 protein ubiquitination and degradation in response to interleukin-1beta. J Biol Chem. 2011; 286:32064–73. [PubMed: 21708940]

FABIAN JR, DAAR IO, MORRISON DK. Critical tyrosine residues regulate the enzymatic and biological activity of Raf-1 kinase. Mol Cell Biol. 1993; 13:7170–9. [PubMed: 7692235]

FAURE E, EQUILS O, SIELING PA, THOMAS L, ZHANG FX, KIRSCHNING CJ, POLENTARUTTI N, MUZIO M, ARDITI M. Bacterial lipopolysaccharide activates NF-kappaB through toll-like receptor 4 (TLR-4) in cultured human dermal endothelial cells. Differential expression of TLR-4 and TLR-2 in endothelial cells. J Biol Chem. 2000; 275:11058–63. [PubMed: 10753909]

FELEDER C, PERLIK V, BLATTEIS CM. Preoptic nitric oxide attenuates endotoxic fever in guinea pigs by inhibiting the POA release of norepinephrine. Am J Physiol Regul Integr Comp Physiol. 2007; 293:R1144–51. [PubMed: 17584955]

FRIDE E. Endocannabinoids in the central nervous system--an overview. Prostaglandins Leukot Essent Fatty Acids. 2002; 66:221–33. [PubMed: 12052038]

GANDO S, KAMEUE T, MATSUDA N, SAWAMURA A, HAYAKAWA M, KATO H. Systemic inflammation and disseminated intravascular coagulation in early stage of ALI and ARDS: role of neutrophil and endothelial activation. Inflammation. 2004; 28:237–44. [PubMed: 15673166]

GONG P, ANGELINI DJ, YANG S, XIA G, CROSS AS, MANN D, BANNERMAN DD, VOGEL SN, GOLDBLUM SE. TLR4 signaling is coupled to SRC family kinase activation, tyrosine phosphorylation of zonula adherens proteins, and opening of the paracellular pathway in human lung microvascular endothelia. J Biol Chem. 2008; 283:13437–49. [PubMed: 18326860]

GU Z, FONSECA V, HAI CM. Nicotinic acetylcholine receptor mediates nicotine-induced actin cytoskeletal remodeling and extracellular matrix degradation by vascular smooth muscle cells. Vascul Pharmacol. 2013; 58:87–97. [PubMed: 22940282]

GUHA M, O'CONNELL MA, PAWLINSKI R, HOLLIS A, MCGOVERN P, YAN SF, STERN D, MACKMAN N. Lipopolysaccharide activation of the MEK-ERK1/2 pathway in human monocytic cells mediates tissue factor and tumor necrosis factor alpha expression by inducing Elk-1 phosphorylation and Egr-1 expression. Blood. 2001; 98:1429–39. [PubMed: 11520792]

HERKENHAM M, LYNN AB, JOHNSON MR, MELVIN LS, DE COSTA BR, RICE KC. Characterization and localization of cannabinoid receptors in rat brain: a quantitative in vitro autoradiographic study. J Neurosci. 1991; 11:563–83. [PubMed: 1992016]

HIRASAWA M, SCHWAB Y, NATAH S, HILLARD CJ, MACKIE K, SHARKEY KA, PITTMAN QJ. Dendritically released transmitters cooperate via autocrine and retrograde actions to inhibit afferent excitation in rat brain. J Physiol. 2004; 559:611–24. [PubMed: 15254151]

HOTCHKISS RS, KARL IE. The pathophysiology and treatment of sepsis. N Engl J Med. 2003; 348:138–50. [PubMed: 12519925]

IBRAHIM BM, ABDEL-RAHMAN AA. Role of brainstem GABAergic signaling in central cannabinoid receptor evoked sympathoexcitation and pressor responses in conscious rats. Brain Res. 2011; 1414:1–9. [PubMed: 21840505]

JOHNSON A, FERRO TJ. Nitrovasodilator repletion increases TNF-alpha-induced pulmonary edema. J Appl Physiol. 1996; 80:2151–5. [PubMed: 8806924]

KADOI Y, GOTO F. Effects of AM281, a cannabinoid antagonist, on circulatory deterioration and cytokine production in an endotoxin shock model: comparison with norepinephrine. J Anesth. 2006; 20:284–9. [PubMed: 17072693]

KAGAN JC, SU T, HORNG T, CHOW A, AKIRA S, MEDZHITOV R. TRAM couples endocytosis of Toll-like receptor 4 to the induction of interferon-beta. Nat Immunol. 2008; 9:361–8. [PubMed: 18297073]

KATHMANN M, FLAU K, REDMER A, TRANKLE C, SCHLICKER E. Cannabidiol is an allosteric modulator at mu- and delta-opioid receptors. Naunyn Schmiedebergs Arch Pharmacol. 2006; 372:354–61. [PubMed: 16489449]

KAWAGOE T, SATO S, MATSUSHITA K, KATO H, MATSUI K, KUMAGAI Y, SAITOH T, KAWAI T, TAKEUCHI O, AKIRA S. Sequential control of Toll-like receptor-dependent responses by IRAK1 and IRAK2. Nat Immunol. 2008; 9:684–91. [PubMed: 18438411]

LAVIOLETTE SR, GRACE AA. Cannabinoids Potentiate Emotional Learning Plasticity in Neurons of the Medial Prefrontal Cortex through Basolateral Amygdala Inputs. J Neurosci. 2006; 26:6458–68. [PubMed: 16775133]

LEE SH, FOLDY C, SOLTESZ I. Distinct endocannabinoid control of GABA release at perisomatic and dendritic synapses in the hippocampus. J Neurosci. 2010; 30:7993–8000. [PubMed: 20534847]

LIAUDET L, PACHER P, MABLEY JG, VIRAG L, SORIANO FG, HASKO G, SZABO C. Activation of poly(ADP-Ribose) polymerase-1 is a central mechanism of lipopolysaccharide-induced acute lung inflammation. Am J Respir Crit Care Med. 2002; 165:372–7. [PubMed: 11818323]

LINDBERG D, CHEN P, LI C. Conditional viral tracing reveals that steroidogenic factor 1-positive neurons of the dorsomedial subdivision of the ventromedial hypothalamus project to autonomic centers of the hypothalamus and hindbrain. J Comp Neurol. 2013; 521:3167–90. [PubMed: 23696474]

LIU A, GONG P, HYUN SW, WANG KZ, CATES EA, PERKINS D, BANNERMAN DD, PUCHE AC, TOSHCHAKOV VY, FANG S, AURON PE, VOGEL SN, GOLDBLUM SE. TRAF6 protein couples Toll-like receptor 4 signaling to Src family kinase activation and opening of paracellular pathway in human lung microvascular endothelia. J Biol Chem. 2012; 287:16132–45. [PubMed: 22447928]

LOMAKINA EB, WAUGH RE. Adhesion between human neutrophils and immobilized endothelial ligand vascular cell adhesion molecule 1: divalent ion effects. Biophys J. 2009; 96:276–84. [PubMed: 19134480]

MADDEN CJ, TUPONE D, CANO G, MORRISON SF. alpha2 Adrenergic receptor-mediated inhibition of thermogenesis. J Neurosci. 2013; 33:2017–28. [PubMed: 23365239]

MARTELLI D, YAO ST, MANCERA J, MCKINLEY MJ, MCALLEN RM. Reflex control of inflammation by the splanchnic anti-inflammatory pathway is sustained and independent of anesthesia. Am J Physiol Regul Integr Comp Physiol. 2014a; 307:R1085–91. [PubMed: 25163921]

MARTELLI D, YAO ST, MCKINLEY MJ, MCALLEN RM. Reflex control of inflammation by sympathetic nerves, not the vagus. J Physiol. 2014b; 592:1677–86. [PubMed: 24421357]

MATSUDA LA, BONNER TI, LOLAIT SJ. Localization of cannabinoid receptor mRNA in rat brain. J Comp Neurol. 1993; 327:535–50. [PubMed: 8440779]

NAKAYAMA K, OTA Y, OKUGAWA S, ISE N, KITAZAWA T, TSUKADA K, KAWADA M, YANAGIMOTO S, KIMURA S. Raf1 plays a pivotal role in lipopolysaccharide-induced activation of dendritic cells. Biochem Biophys Res Commun. 2003; 308:353–60. [PubMed: 12901876]

NANCE DM, SANDERS VM. Autonomic innervation and regulation of the immune system (1987–2007). Brain Behav Immun. 2007; 21:736–45. [PubMed: 17467231]

PAI AB, PATEL H, PROKOPIENKO AJ, ALSAFFAR H, GERTZBERG N, NEUMANN P, PUNJABI A, JOHNSON A. Lipoteichoic acid from Staphylococcus aureus induces lung endothelial cell barrier dysfunction: role of reactive oxygen and nitrogen species. PLoS One. 2012; 7:e49209. [PubMed: 23166614]

ROSAS-BALLINA M, TRACEY KJ. Cholinergic control of inflammation. J Intern Med. 2009; 265:663–79. [PubMed: 19493060]

SAPER CB, LOEWY AD, SWANSON LW, COWAN WM. Direct hypothalamo-autonomic connections. Brain Res. 1976; 117:305–12. [PubMed: 62600]

SAWA Y, UEKI T, HATA M, IWASAWA K, TSURUGA E, KOJIMA H, ISHIKAWA H, YOSHIDA S. LPS-induced IL-6, IL-8, VCAM-1, and ICAM-1 expression in human lymphatic endothelium. J Histochem Cytochem. 2008; 56:97–109. [PubMed: 17938282]

SCHULTE K, STEINGRUBER N, JERGAS B, REDMER A, KURZ CM, BUCHALLA R, LUTZ B, ZIMMER A, SCHLICKER E. Cannabinoid CB1 receptor activation, pharmacological blockade, or genetic ablation affects the function of the muscarinic auto- and heteroreceptor. Naunyn Schmiedebergs Arch Pharmacol. 2012; 385:385–96. [PubMed: 22215206]

SIMONS RK, JUNGER WG, LOOMIS WH, HOYT DB. Acute lung injury in endotoxemic rats is associated with sustained circulating IL-6 levels and intrapulmonary CINC activity and neutrophil recruitment--role of circulating TNF-alpha and IL-beta? Shock. 1996; 6:39–45. [PubMed: 8828083]

SU X, MATTHAY MA, MALIK AB. Requisite role of the cholinergic alpha7 nicotinic acetylcholine receptor pathway in suppressing Gram-negative sepsis-induced acute lung inflammatory injury. J Immunol. 2010; 184:401–10. [PubMed: 19949071]

SU X, ROBRIQUET L, FOLKESSON HG, MATTHAY MA. Protective effect of endogenous beta-adrenergic tone on lung fluid balance in acute bacterial pneumonia in mice. Am J Physiol Lung Cell Mol Physiol. 2006; 290:L769–L776. [PubMed: 16284214]

SZABO B, SCHLICKER E. Effects of cannabinoids on neurotransmission. Handb Exp Pharmacol. 2005:327–65. [PubMed: 16596780]

TOGBE D, SCHNYDER-CANDRIAN S, SCHNYDER B, COUILLIN I, MAILLET I, BIHL F, MALO D, RYFFEL B, QUESNIAUX VF. TLR4 gene dosage contributes to endotoxin-induced acute respiratory inflammation. J Leukoc Biol. 2006; 80:451–7. [PubMed: 16809643]

TOUBIANA J, COURTINE E, PENE F, VIALLON V, ASFAR P, DAUBIN C, ROUSSEAU C, CHENOT C, OUAAZ F, GRIMALDI D, CARIOU A, CHICHE JD, MIRA JP. IRAK1 functional genetic variant affects severity of septic shock. Crit Care Med. 2010; 38:2287–94. [PubMed: 20890200]

VAN AMERSFOORT ES, VAN BERKEL TJ, KUIPER J. Receptors, mediators, and mechanisms involved in bacterial sepsis and septic shock. Clin Microbiol Rev. 2003; 16:379–414. [PubMed: 12857774]

VARGA K, WAGNER JA, BRIDGEN DT, KUNOS G. Platelet- and macrophage-derived endogenous cannabinoids are involved in endotoxin-induced hypotension. FASEB J. 1998; 12:1035–44. [PubMed: 9707176]

VILLANUEVA A, YILMAZ SM, MILLINGTON WR, CUTRERA RA, STOUFFER DG, PARSONS LH, CHEER JF, FELEDER C. Central cannabinoid 1 receptor antagonist administration prevents endotoxic hypotension affecting norepinephrine release in the preoptic anterior hypothalamic area. Shock. 2009; 32:614–20. [PubMed: 19295473]

VOGEL SN, FITZGERALD KA, FENTON MJ. TLRs: differential adapter utilization by toll-like receptors mediates TLR-specific patterns of gene expression. Mol Interv. 2003; 3:466–77. [PubMed: 14993454]

WANG Y, PEREIRA EF, MAUS AD, OSTLIE NS, NAVANEETHAM D, LEI S, ALBUQUERQUE EX, CONTI-FINE BM. Human bronchial epithelial and endothelial cells express alpha7 nicotinic acetylcholine receptors. Mol Pharmacol. 2001; 60:1201–9. [PubMed: 11723227]

YILMAZ MS, GOKTALAY G, MILLINGTON WR, MYER BS, CUTRERA RA, FELEDER C. Lipopolysaccharide-induced hypotension is mediated by a neural pathway involving the vagus nerve, the nucleus tractus solitarius and alpha-adrenergic receptors in the preoptic anterior hypothalamic area. J Neuroimmunol. 2008a; 203:39–49. [PubMed: 18653249]

YILMAZ MS, MILLINGTON WR, FELEDER C. The preoptic anterior hypothalamic area mediates initiation of the hypotensive response induced by LPS in male rats. Shock. 2008b; 29:232–7. [PubMed: 18386391]

Highlights

- Brain injection of rimonabant prevents LPS-induced pulmonary hemodynamic changes.
- Brain injection of rimonabant prevents LPS-induced pulmonary edema.
- Brain injection of rimonabant alters LPS-induced TLR4 signaling.
- Brain injection of rimonabant alters LPS-induced pulmonary inflammatory markers.

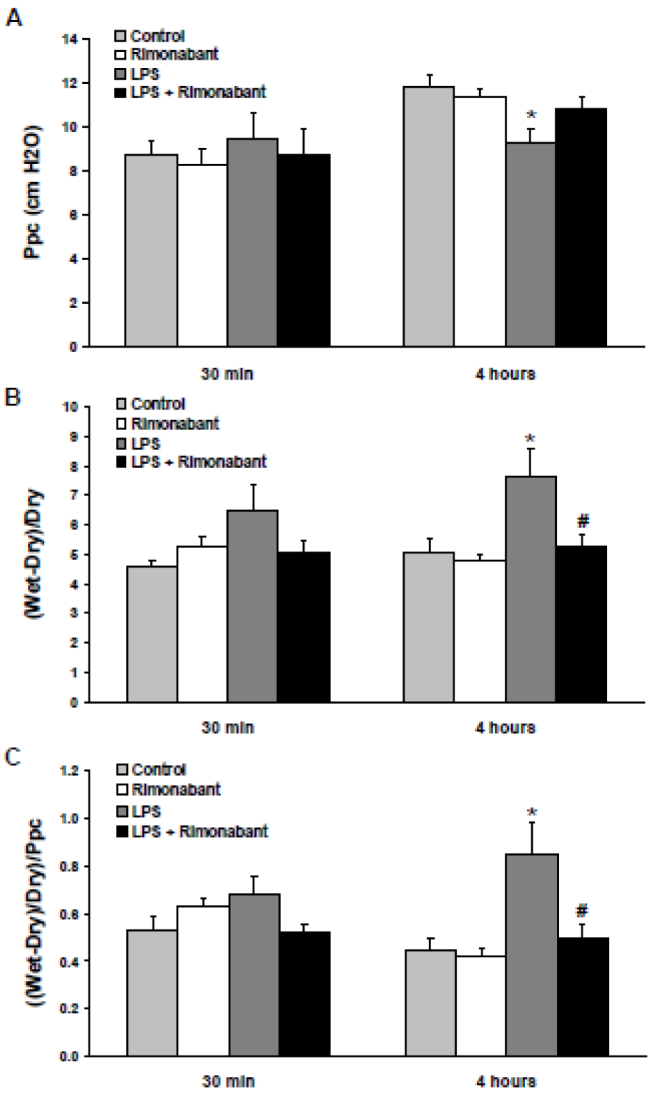

Figure 1. Rimonabant prevents the pulmonary hemodynamic changes and pulmonary fluid accumulation following systemic LPS

Following a 30 minute or 4 hour exposure to 5mg/kg systemic LPS dose (IV) with or without intracerebroventricular rimonabant pre-treatment (500 ng in 0.5 μl saline + 2.5% DSMO), the lungs and heart of rats were excised and suspended from an isolated-lung apparatus, ventilated with room air, perfused with Ringer's/BSA solution (pH 7.4), and maintained at 37 °C. ***A)*** The pulmonary artery and left atrial appendage were cannulated to measure pulmonary arterial pressure and to maintain pulmonary venous pressure at 2.9 mmHg, respectively. Pulmonary capillary pressure (Ppc) was estimated using the double occlusion method after 15 minutes of perfusion. ***B)*** Following the pulmonary hemodynamic measurements, the lungs were separated into left and right halves. Left lungs were weighed in their wet state and subsequently oven dried for three days. The left lung wet to dry weight ratio was calculated by ((wet weight – dry weight)/dry weight) ((W-D)/D). ***C)*** The (W-D)/D ratio of each lung was indexed to the Ppc obtained for that lung as ((W-D)/D)/Ppc. Data are

mean ± S.E.M. Significance was at $P<0.05$. * = significantly different from respective control. # = significantly different from its LPS-only group.

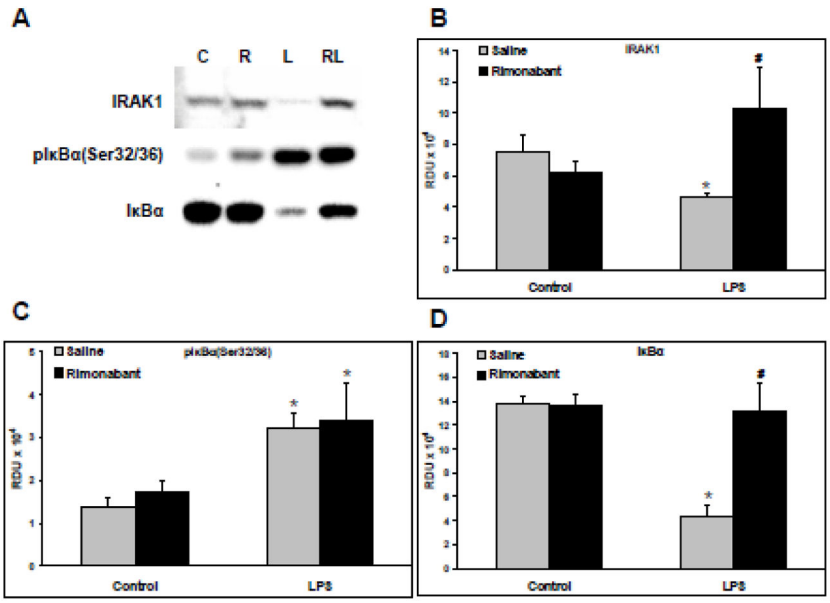

Figure 2. Rimonabant modulates TLR4 signaling following systemic LPS injection

Following hemodynamic measurements, lungs isolated from rats exposed to systemic LPS (5mg/kg) for 30 minutes with or without intracerebroventricular rimonabant pretreatment (500 ng in 0.5 μl saline + 2.5% DSMO), were separated into left and right halves. Right lungs were homogenized, and supernatants, 20 μg/lane, were Western blotted. ***A)*** Representative blots are shown of IRAK1, phospho-IκBα$^{Ser\ 32/36}$, and IκBα; **C**=control, **R**=rimonabant, **L**=LPS, **RL**=rimonabant pretreatment + LPS. ***B)*** The Western blot band densities of IRAK1 in relative density units (RDU). ***C)*** The Western blot band densities of phospho-IκBα$^{Ser\ 32/36}$ in RDU. ***D)*** The Western blot band densities of IκBα$^{Ser\ 32/36}$ in RDU. Data are mean ± S.E.M. Significance was at $P<0.05$. * = significantly different from control. # = significantly different from its LPS-only group.

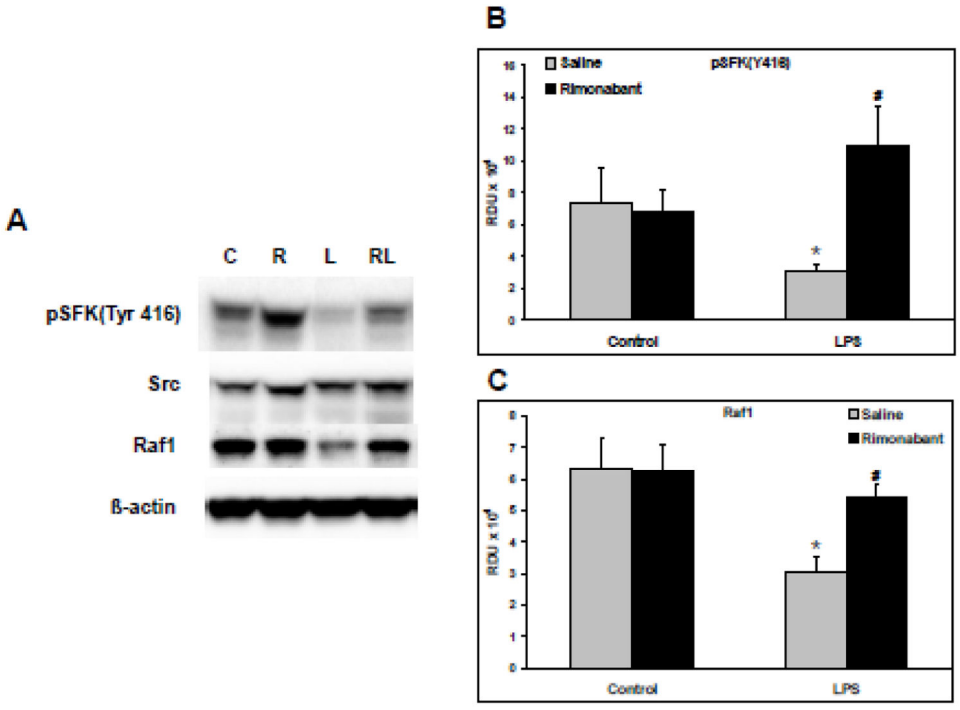

Figure 3. Rimonabant modulates phospho-SFK^{Tyr416} and RAF1 following systemic LPS injection

Following hemodynamic measurements, lungs isolated from rats exposed to systemic LPS (5mg/kg) for 30 minutes with or without intracerebroventricular rimonabant pretreatment (500 ng in 0.5 μl saline + 2.5% DSMO), were separated into left and right halves. Right lungs were homogenized, and supernatants, 20 μg/lane, were Western blotted. ***A)*** Representative blots are shown for phospho-SFK$^{Tyr\ 416}$, *total Src, RAF1, and β-actin*. **C**=control, **R**=rimonabant, **L**=LPS and **RL**=rimonabant pretreatment + LPS. ***B)*** The Western blot band densities of phospho-Src$^{Tyr\ 416}$ in relative density units (RDU). ***C)*** *The Western blot band densities of Raf1 in relative density units (RDU)*. Data are mean ± S.E.M. Significance was at $P<0.05$. * = significantly different from control. # = significantly different from the LPS-only group. $ = significantly different from the ICV rimonabant + LPS group.

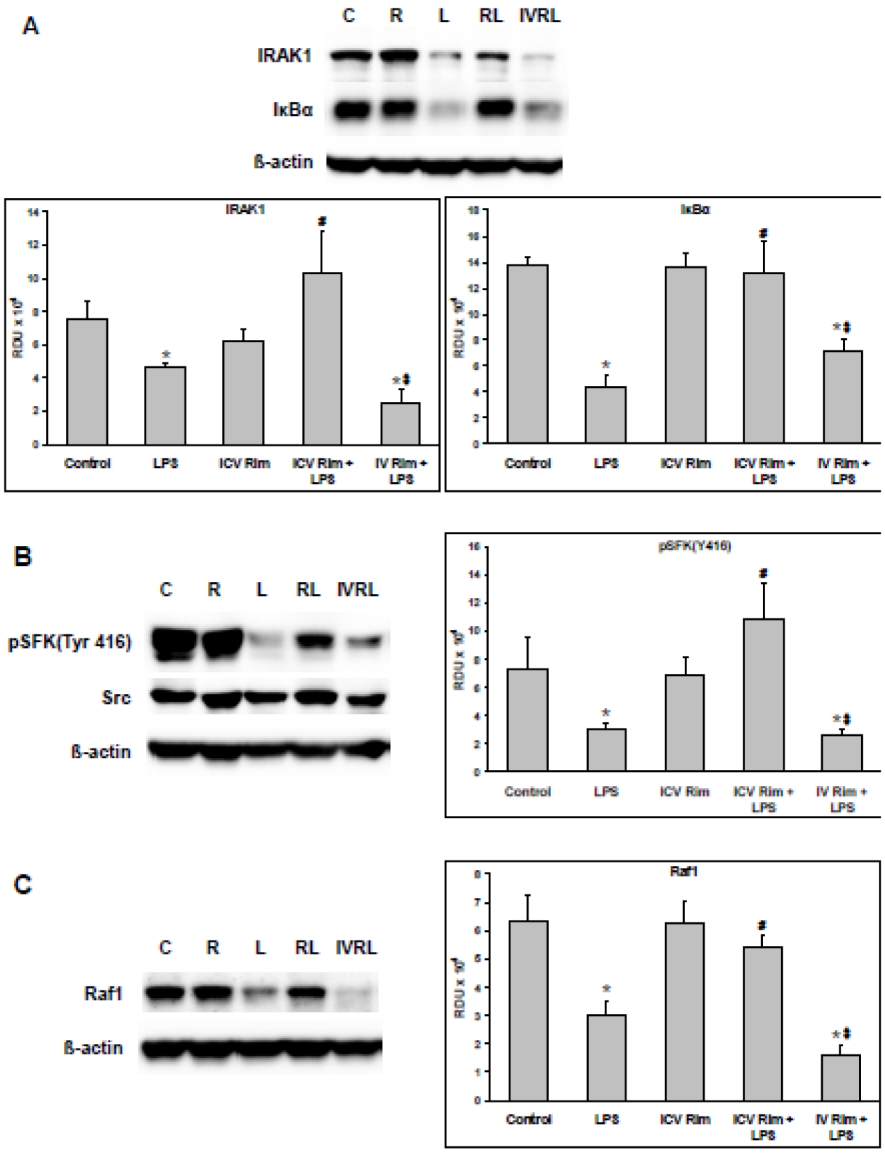

Figure 4. Intravenous rimonabant does not modulate pulmonary LPS effects

Following hemodynamic measurements, lungs isolated from rats exposed to systemic LPS (5mg/kg) for 30 minutes with or without intracerebroventricular or intravenous rimonabant pretreatment (500 ng in 0.5 μl saline + 2.5% DSMO), were separated into left and right halves. Right lungs were homogenized, and supernatants, 20 μg/lane, were Western blotted. The blot lane labels are: **C**=control, **R**=rimonabant, **L**=LPS, **RL**=ICV rimonabant pretreatment + LPS, **IVRL**=IV rimonabant pretreatment + LPS. **A)** Representative blots of IRAK1, IκBα, and β-actin and the Western blot band densities of IRAK1 and IκBα in relative density units (RDU) **B)** Representative blots of phospho-SFK^{Tyr416}, total Src, and β-actin and the Western blot RDU for phospho-SFK^{Tyr416}. **C)** Representative blots of total RAF1 and β-actin and the Western blot RDU for RAF1. Data are mean ± S.E.M. Significance was at $P<0.05$. * = significantly different from control. # = significantly

different from the LPS-only group. $ = significantly different from the ICV rimonabant + LPS group.

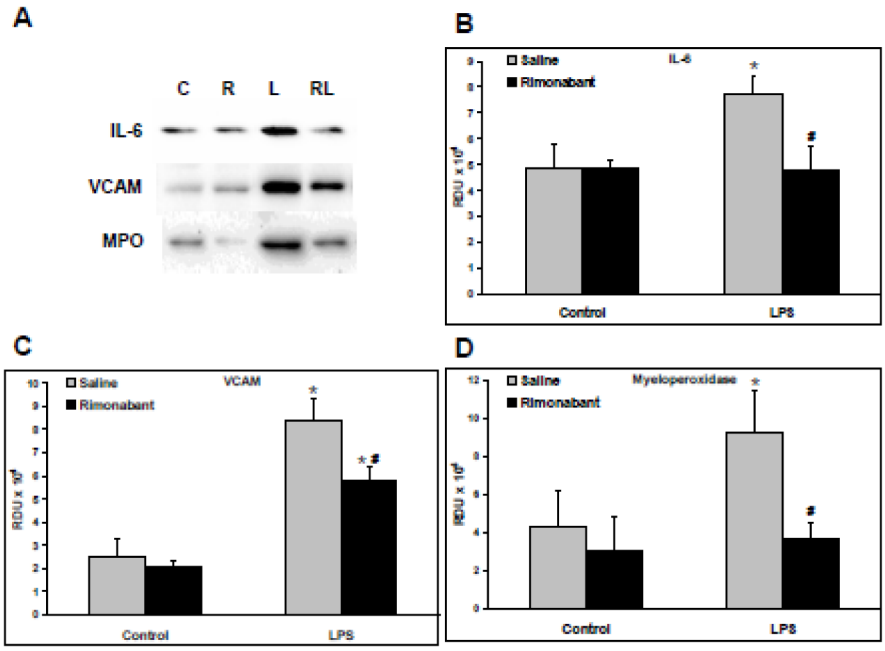

Figure 5. Rimonabant modulates IL-6, VCAM, and MPO expression following systemic LPS injection

Following hemodynamic measurements, lungs isolated from rats exposed to systemic LPS (5mg/kg) for 4 hours with or without intracerebroventricular rimonabant treatment, were separated into left and right halves. Right lungs were homogenized, and supernatants, 20 μg/lane, were Western blotted. ***A)*** Representative blots are shown of IL-6, VCAM, Myeloperoxidase (MPO); **C**=control, **R**=rimonabant, **L**=LPS and **RL**=rimonabant treatments + LPS. ***B)*** The Western blot band densities of IL-6, in relative density units (RDU). ***C)*** The Western blot band densities of VCAM, in RDU. ***D)*** The Western blot band densities of MPO in RDU. Data are mean ± S.E.M. Significance was at $P<0.05$. * = significantly different from control. # = significantly different from its LPS-only group.